Original scientific paper

FRICTION UNDER LARGE-AMPLITUDE
NORMAL OSCILLATIONS

Mikhail Popov[1,2]

[1]Technische Universität Berlin, Germany
[2]National Research Tomsk State University, Russia

Abstract. *Building on a recently proposed contact-mechanical theory of friction control by external vibration, the case of large-amplitude normal oscillation is revisited. It is shown that the coefficient of friction can be expressed in particularly simple form if the waveform of the displacement oscillation is triangular or rectangular, and the contact stiffness is constant. The latter requirement limits the scope of the exact solutions to contacts between a plane and a flat-ended cylinder or a curved shape with a wear flat, but the adopted methodology also enables efficient numerical solution in more general cases.*

Key words: *Contact Mechanics, Vibration, Control of Friction, Large Amplitudes, Sliding Friction*

1. INTRODUCTION

The ability of externally applied vibration to substantially reduce both static and sliding friction is well known and enjoys many practical applications. The classical examples of wire drawing [1,2] and metal forming [3,4] deserve mention, but a thorough review is outside the scope of this paper. While the effect has attracted a fair amount of research, most of the works are of an experimental, application-oriented nature [5-7], and proposed models are at best semi-empirical [8]. For this reason, no consensus has been established concerning the theoretical underpinnings of the phenomenon. A possible physical model based on macroscopic contact mechanics was recently proposed by the author and colleagues [9]. The mechanism of force reduction in this model is based on the observation that stick-slip can arise in an oscillating contact under suitable conditions, if the compliance of the contact is taken into account. During the stick phases the lateral

force is by definition subcritical (i.e. less than what is required to sustain sliding), and therefore lowers the average friction force. Multiple extensions of this model have since been published and were reviewed in a recent paper [10]. Here, the same approach is used to analyze the case of large-amplitude normal oscillation, when the amplitude is larger than the mean indentation and the body starts to "jump" over the plane.

2. MODEL

For a complete description of the model the reader is referred to previous publications [9,10], but a short overview is provided here for convenience. First and foremost, it is assumed that the contact is quasistatic and that the contact stiffness is independent of indentation depth. Both assumptions are nonessential for the model as such, but are required for analytical calculations. Together, they allow us to treat the contact as a single linearly elastic massless spring (Fig. 1) with normal and lateral stiffness k_z and k_x, respectively. If the modeled contact is a flat-ended cylinder with radius a, the stiffness values are given by:

$$k_z = 2E^* a \quad \text{where} \quad \frac{1}{E^*} = \frac{1-v_1^2}{E_1} + \frac{1-v_2^2}{E_2}$$

$$k_x = 2G^* a \quad \text{where} \quad \frac{1}{G^*} = \frac{2-v_1}{4G_1} + \frac{2-v_2}{4G_2}$$

(1)

with E_i, G_i being the elastic and shear moduli of the contacting bodies and v_i their Poisson numbers.
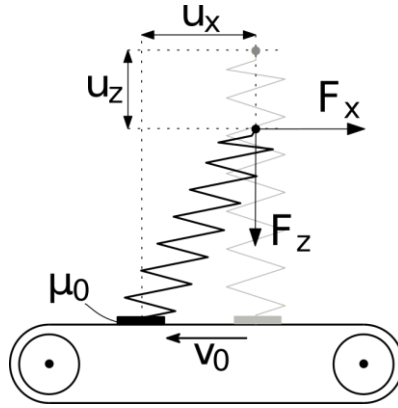

Fig. 1 A single massless spring, which serves as a minimal model of a sliding frictional contact. The sliding velocity is constant, while the vertical coordinate oscillates. Amontons friction with the constant coefficient of friction μ_0 is assumed in the contact.

The spring is pulled with a constant velocity v_0 while also being subjected to a normal oscillation that is parametrized as

$$u_z(t) = \bar{u}_z + A_z w(ft)$$

(2)

where $\bar{u}_z$ is the mean indentation, A_z the amplitude, f the frequency and w a zero-mean, unit-amplitude waveform. The lateral displacement u_x is the primary unknown of the system.

When the contact point is in a sliding state, its velocity can be shown to be

$$\dot{u}_x(t) = \mu_0 \frac{k_z}{k_x} A_z f w'(ft) \tag{3}$$

The contact transitions from slip to stick when this velocity vanishes. The point of stick onset $\varphi_1 = ft_1$ can therefore be written as:

$$\varphi_1 = (w')^{-1}(\beta) \tag{4}$$

where β is one of the dimensionless variables that parametrize the behavior of the system:

$$\alpha = \frac{A_z}{\bar{u}_z}, \qquad \beta = \frac{k_x v_0}{\mu_0 k_z A_z f}, \qquad \varphi = ft \tag{5}$$

The Eq. (4) does not necessarily have solutions. For stick-slip to be present, it is necessary that

$$\beta < \max_{\varphi} w'(\varphi) = \beta_c \tag{6}$$

where β_c is the maximum positive gradient of the oscillation waveform. If the dimensionless velocity β exceeds this threshold value, stick-slip becomes impossible and the macroscopic coefficient of friction $\bar{\mu}$ is the same as the intrinsic coefficient of friction μ_0. Otherwise it is reduced by some amount that depends on α, β and the shape of w.

If condition (6) is satisfied and stick is initiated, the spring continues stretching with the constant velocity v_0 and the lateral spring force therefore increases linearly with time:

$$F_{\text{stick}}(t) = \mu_0 F_z(t_1) + k_x v_0(t - t_1) \tag{7}$$

This continues while the stick condition $F_{\text{stick}} < \mu_0 F_z(t)$ holds. Substituting $F_z = k_z u_z$ and rearranging gives the end of the stick phase φ_2 in implicit form:

$$\beta(\varphi_2 - \varphi_1) = w(\varphi_2) - w(\varphi_1) \tag{8}$$

The stick-slip process is visualized in Fig. 2.

The macroscopic friction force $\langle F_x \rangle$ is computed by integrating $F_x(t)$ over both the slip and stick periods:

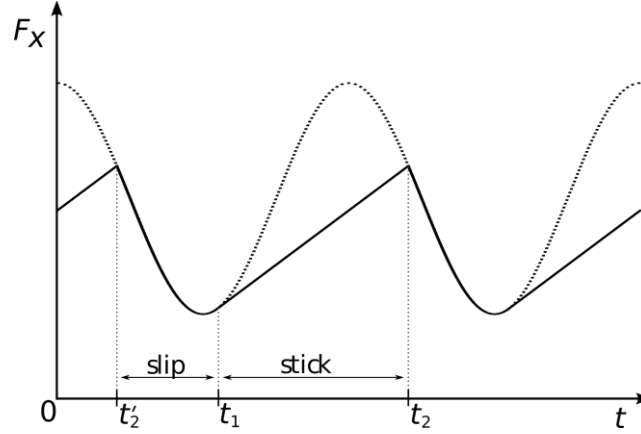$$\langle F_x \rangle = \frac{1}{T} \int_0^T F_x(t) \, dt \tag{9}$$

Fig. 2 Stick and slip under the influence of a harmonic oscillation. The dotted line represents the tangential force as it would be in pure slip, $F_{\text{slip}} = \mu_0 F_z(t)$. The solid line is the actual tangential force in the presence of stick-slip. The stick phases are the straight segments, e.g. between t_1 and t_2, while slip phases are the sinusoidal segments, e.g. between t_2' and t_1, repeating periodically. Note that $F_x \leq F_{\text{slip}}$ everywhere, which is the origin of friction reduction in our model.

Since F_x only differs from $\mu_0 F_z$ during the stick phase, it is actually more convenient to determine the absolute force reduction $\Delta F_x = \langle \mu_0 F_z \rangle - \langle F_x \rangle$:

$$\Delta F_x = \frac{1}{T} \int_{t_1}^{t_2} \left(\mu_0 F_z(t) - F_{\text{stick}}(t) \right) \mathrm{d}t \tag{10}$$

After expanding and rearranging, it is found that ΔF_x can be expressed as

$$\Delta F_x = \mu_0 k_z A_z \Psi_w(\beta) \tag{11}$$

where Ψ_w is a dimensionless "reduction function" that is specific to the waveform w:

$$\Psi_w(\beta) = \int_{\varphi_1}^{\varphi_2} \left(w(\varphi) - w(\varphi_1) - \beta(\varphi - \varphi_1) \right) \mathrm{d}\varphi \tag{12}$$

The macroscopic coefficient of friction $\bar{\mu}$ can then be recovered through

$$\bar{\mu} = \frac{\langle \mu_0 F_z \rangle - \Delta F_x}{\langle F_z \rangle} = \mu_0 - \frac{\Delta F_x}{k_z \bar{u}_z} = \mu_0 \left(1 - \alpha \Psi_w(\beta) \right) \tag{13}$$

This puts the dependence into a very simple form, with most of the complexity contained in a function of one argument, $\Psi_w(\beta)$. This function, however, needs to be determined numerically in most cases.

This concludes our whirlwind tour of the model framework that will be used in the sequel. A less hurried presentation can be found in [10].

3. LARGE AMPLITUDES

In the preceding discussion it was implicitly assumed that the amplitude A_z is smaller than the mean indentation $\bar{u}_z$, so that the bodies are permanently in contact and the normal force is non-negative. The purpose of this paper is to extend the analysis to $A_z > |\bar{u}_z|$, that is, cases where the bodies lose contact periodically. Equivalently, $-A_z < \bar{u}_z < A_z$, where we have excluded the trivial no-contact case. This form also makes evident the need for a small re-parametrization:

$$\gamma = \frac{1}{\alpha} = \frac{\bar{u}_z}{A_z} \tag{14}$$

which avoids the singularity at $\bar{u}_z = 0$.

The first thing to note about the jumping case is that the static coefficient of friction is always zero, because the contact obviously cannot sustain a lateral force while it is "in the air", and slow creep will therefore be present at arbitrarily small pulling forces. If measurements of the static coefficient of friction under normal oscillation do not go to zero at suitably large amplitudes, this probably indicates a misalignment in the measurement apparatus.

The second thing to note is that, in general, the simplicity of Eq. (13) can no longer be maintained. The clean separation between α and β is only possible because the stick-slip process is completely independent of mean indentation, so long as the normal force F_z is positive throughout. However, when $u_z(t)$ becomes negative in the jumping case, this causes F_z to become "clipped" at zero (assuming no adhesion). This destroys the invariance w.r.t. $\bar{u}_z$, because the waveform w effectively becomes "cut off", and has to be renormalized to maintain the properties of zero mean and unit amplitude. Thus, $w(\varphi)$ should properly be $w(\gamma,\varphi)$ in the jumping case. Overall, this leads us to expect the coefficient of friction to be a nonlinear function of two parameters (in addition to the waveform dependence):

$$\bar{\mu}_{\mathrm{jmp}} = \mu_0 g_w\left(\beta,\gamma\right) \tag{15}$$

In general, the function g needs to be computed numerically. There are, however, a few cases of some practical importance that can be treated analytically. These include square and triangle waves, for which solutions can be obtained in closed form due to their simplicity; and certain self-similar oscillations, for which asymptotic behavior can be deduced. These cases are considered next.

3.1 Special case 1: Sawtooth and triangle wave

Of the possible waveforms with triangular shape, here we consider the left-leaning sawtooth function (stl), the right-leaning sawtooth function (str) and the symmetric triangle wave (tri). The normalized functions w for these waveforms can be defined on the unit interval (with periodic extension understood) as:

$$w_{\text{stl}} = 1 - 2\varphi$$
$$w_{\text{str}} = 2\varphi - 1 \tag{16}$$
$$w_{\text{tri}} = \begin{cases} 4\varphi - 1, & \varphi < 1/2 \\ 3 - 4\varphi, & \varphi > 1/2 \end{cases}$$

From geometrical considerations (which come down to determining the area between the waveform and a straight line with the slope β as in Fig. 2), it is easy to show that the corresponding reduction functions $\Psi_w(\beta)$ in the simple non-jumping case are given by:

$$\Psi_{\text{str}}(\beta) = 1 - \frac{\beta}{2}, \quad \Psi_{\text{stl}}(\beta) = \frac{2}{2+\beta}, \quad \Psi_{\text{tri}}(\beta) = \frac{4-\beta}{4+\beta} \tag{17}$$

The triangular waves have the unique property that clipping the waveform does not affect the coefficient of friction. To appreciate this, refer once again to Fig. 2. The coefficient of friction is given by the ratio of the area under F_x to the area under $\mu_0 F_z$. This ratio changes continuously as the waveform is clipped from below by increasingly large amplitudes. If the waveform is triangular, however, then the only effect from the cutoff is that the ramp of the stick phase starts later and later (in the point of first contact). The area ratio is not affected, which means that the coefficient of friction remains constant, despite the fact that Ψ_w formally depends on γ. This means that, for triangular waves,

$$\bar{\mu}(\beta, \gamma < 1) = \bar{\mu}(\beta, \gamma = 1) = \mu_0 \left(1 - \Psi_w(\beta)\right) \tag{18}$$

Using the reduction functions given in Eq. (17), this provides the following simple results for the coefficient of friction under large-amplitude oscillation:

$$\bar{\mu}_{\text{str}}(\beta) = \mu_0 \frac{\beta}{2}, \quad \bar{\mu}_{\text{stl}}(\beta) = \mu_0 \frac{\beta}{2+\beta}, \quad \bar{\mu}_{\text{tri}}(\beta) = \mu_0 \frac{2\beta}{4+\beta} \tag{19}$$

3.2 Special case 2: Self-similar waveforms, Square wave

The triangular waves are a special case of what could be termed *self-similar* waveforms. By this we mean that a cut-off waveform can be rescaled in such a fashion as to be identical to the original waveform. Assuming that the waveform is also *convex* ensures that stick is precipitated in the point of first contact, as in the case of the triangular wave. This means that the stick-slip graph of a cut-off waveform can be rescaled (together with the stick ramp) to have the same area ratio – and therefore the same coefficient of friction – as the same waveform at another cutoff. Of course, this rescaling also changes the slope β, which must be adjusted accordingly. Usually, it is convenient to choose the coefficient of friction at $\gamma = 1$ as a reference point, so that the large-amplitude coefficient of friction of a self-similar waveform can be expressed as:

$$\bar{\mu}(\beta, \gamma) = \mu_0 \left(1 - \Psi_w\left(\xi(\beta, \gamma)\right)\right) \tag{20}$$

The function ξ which provides the remapping of β is specific to the waveform.

After the triangle, the next-simplest example of a self-similar waveform is the square wave, which alternates between 1 and -1 in equal intervals. It is easy to show that the remapping function for such an oscillation is given by:

$$\xi_{\text{sqr}}(\beta, \gamma) = \frac{2\beta}{1+\gamma} \tag{21}$$

Using this mapping and the reduction function Ψ_{sqr} of the square wave (see Eq. (36) in [10]), the coefficient of friction under large-amplitude square wave oscillations can be written as:

$$\frac{\bar{\mu}_{\text{sqr}}}{\mu_0} = \begin{cases} \dfrac{\beta}{4(1+\gamma)}, & \beta < 2(1+\gamma) \\[2ex] 1 - \dfrac{1+\gamma}{\beta}, & \beta > 2(1+\gamma) \end{cases} \tag{22}$$

This result is shown in Fig. 3 for the entire range of γ from 1 (starting to separate) to -1 (barely touching).
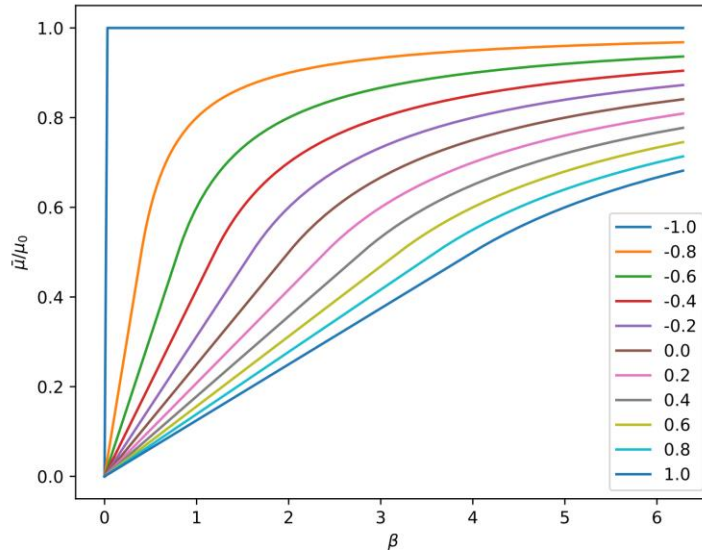

Fig. 3 Coefficient of friction under large-amplitude square wave oscillations with 11 different normalized indentations γ covering the entire jumping range from -1 to 1.

The concept of self-similar waveforms also applies to the harmonic oscillation, to a limited extent. While the entire sine wave is not self-affine according to our definition, it can be approximated piecewise by a parabola over some of its domain. Since the parabola is indeed a self-affine function, we can expect the coefficient of friction under harmonic oscillation to have the described behavior *asymptotically*, although it will not be valid for values of γ close to 1. The remapping function in this case can be shown to be

$$\xi_2(\beta,\gamma) = \beta\sqrt{\frac{1+\gamma_0}{1+\gamma}} \tag{23}$$

where γ_0 is the value of γ at the point where the self-affine scaling behavior started. More generally, for a waveform that can be asymptotically approximated by a power law φ^n, the corresponding remapping can be shown to be

$$\xi_n(\beta,\gamma) = \beta\left(\frac{1+\gamma_0}{1+\gamma}\right)^{1/n} \tag{24}$$

3.3 Numerical example: Harmonic oscillation

As an example of asymptotic scaling, Fig. 4 shows numerically determined coefficients of friction under large-amplitude harmonic oscillation. One thing to note is that for γ in the range of approximately -0.2 to 1, the coefficient of friction depends only weakly on γ, with all curves bunching fairly closely together. The dependence on γ is also non-monotonous in this range, leading to lower coefficients of friction at first (from $\gamma = 1$ to approx. 0.6), and then increasing again (from $\gamma = 0.6$ to -1). The value around $\gamma = -0.3$ is the point from which the remaining part of the cropped waveform can be regarded as roughly parabolical, and the subsequent behavior of the coefficient of friction can be described by the scaling given in Eq. (23). This is also shown in Fig. 4 with black dots.
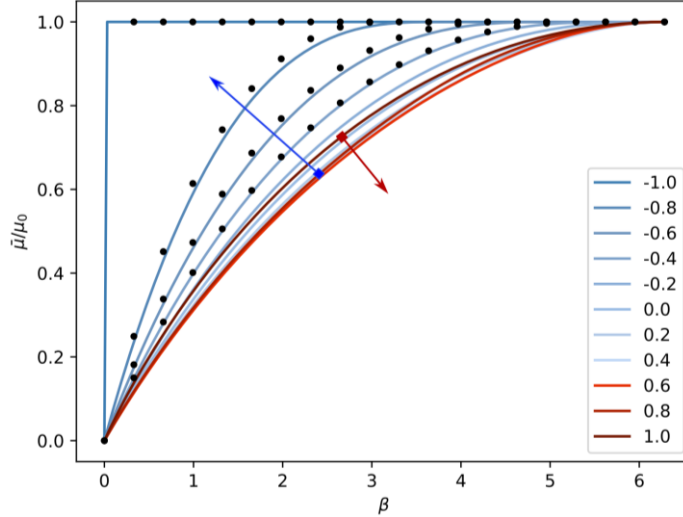

Fig. 4 Numerically computed coefficient of friction under large-amplitude harmonic oscillations with 11 different normalized indentations γ covering the entire jumping range from -1 to 1. Note the non-monotonous dependence on γ: The dark red line corresponds to the critical value $\gamma = 1$, which separates the jumping and non-jumping regions. From there, the coefficient of friction is first reduced with diminishing γ (red lines and arrow) and then increases again (blue lines and arrow) starting somewhere around $\gamma = 0.6$. Black dots indicate the expected scaling behavior according to Eq. (23) relative to $\gamma_0 = -0.3$.

4. CONCLUSIONS

The influence of large-amplitude normal oscillation on sliding friction, which has not previously received much attention in the literature, was analyzed in this work, based on a model proposed by the authors in a previous publication. It was shown that the coefficient of friction in the jumping case depends on the same dimensionless variables as in the low-amplitude case, but in a more complicated fashion. At low amplitudes, the influence of the two main variables, α and β is cleanly separated, while at large amplitudes they become entangled and influence the coefficient of friction in a nontrivial manner. This was demonstrated on the example of the harmonic oscillation, where the amplitude-dependence is non-monotonic and can only be determined numerically. However, some simple cases such as triangular, rectangular and more general self-similar waveforms yield relatively simple results, which allow the coefficient of friction to be expressed either in closed form or as an asymptotic scaling relation.

REFERENCES

1. Siegert, K., Ulmer, J., 2001, *Superimposing ultrasonic waves on the dies in tube and wire drawing*, Journal of Engineering Materials and Technology, 123(4), pp. 517–523.
2. Murakawa, M., Jin, M., 2001, *The utility of radially and ultrasonically vibrated dies in the wire drawing process*, Journal of Materials Processing Technology, 113(1-3), pp. 81-86.
3. Eaves, A., Smith, A., Waterhouse, W., Sansome, D., 1975, *Review of the application of ultrasonic vibrations to deforming metals*, Ultrasonics, 13(4), pp. 162-170.
4. Ashida, Y., Aoyama, H., 2007, *Press forming using ultrasonic vibration*, Journal of Materials Processing Technology, 187, pp. 118-122.
5. Pohlman, R., Lehfeldt, E., 1966, *Influence of ultrasonic vibration on metallic friction*, Ultrasonics, 4(4), pp. 178-185.
6. Godfrey, D., 1967, *Vibration reduces metal to metal contact and causes an apparent reduction in friction*, ASLE transactions, 10(2), pp. 183-192.
7. Chowdhury, M.A., Helali, M., 2008, *The effect of amplitude of vibration on the coefficient of friction for different materials*, Tribology International, 41(4), pp. 307-314.
8. De Wit, C.C., Olsson, H., Satrom, K.J., Lischinsky, P., 1995, *A new model for control of systems with friction*, IEEE Transactions on automatic control, 40(3), pp. 419-425.
9. Popov, M., Popov, V.L., Popov, N.V., 2017, *Reduction of friction by normal oscillations. I. Influence of contact stiffness*, Friction, 5(1), pp. 45-55.
10. Popov, M., 2020, *The influence of vibration on friction: a contact-mechanical perspective*, Frontiers in Mechanical Engineering, 6, pp. 69.